DOI: 10.1021/ic1009626

Inorganic Chemistry
Communication

A Modular Approach to Redox-Active Multimetallic Hydrophobes of Discoid Topology

Frank D. Lesh,[†] Rama Shanmugam,[†] Marco M. Allard,[†] Maurício Lanznaster,[†] Mary Jane Heeg,[†] M. T. Rodgers,[†] Jason M. Shearer,[‡] and Cláudio N. Verani*[,†]

[†]*Department of Chemistry, Wayne State University, Detroit, Michigan 48202, and*
[‡]*Department of Chemistry, University of Nevada, Reno, Nevada 89557*

Received May 14, 2010

A new modular $[Fe^{II}(Fe^{III}L^2)_3](PF_6)_2$ species with discoid (disk-like) topology exhibits redox and surfactant properties and points to a new approach for multimetallic Langmuir film precursors.

The combination of amphiphilic properties with controllable and tunable behavior of transition metal complexes leads to metal-containing surfactants that exhibit interfacial organization, along with variable geometric, charge, redox, optical, and magnetic properties.[1] Considerable progress has been made toward the understanding of this metal ion/amphiphile cooperativity in supramolecular assemblies.[2] Potential high-end uses of metallosurfactants include films for optoelectronics[3] and logic and memory operations[4] and micellar luminescence and electron transfer.[5] Our group is developing precursor metallosurfactants, aiming at the inclusion of ligand- and metal-centered redox activity while preserving the ability to organize into well-ordered films.[6] The current approach involves incorporation of selected metal ions into a phenolate-based headgroup of a designer amphiphile. The phenolate can then be oxidized into a phenoxyl radical. However, because the stabilization of radicals requires the incorporation of *tert*-butyl groups into the headgroup, it has been observed that improved redox properties lead to decreased amphiphilic character and vice versa. Therefore, the development of new topologies that can accommodate both properties becomes highly relevant. Recently, we reported on an $[Fe^{III}L^1]$ species ($(L^1)^{3-}$ is a phenylene−diamine/triphenolate ligand) in which five-coordinate iron(III) centers seem to enhance the formation and reversibility of three consecutive phenolate/phenoxyl processes on the cyclic voltammetric time scale.[7] The related species $[Fe^{III}L^2]$, where $(L^2)^{3-}$ describes a similar phenanthrolinediamine/trisphenolate ligand, served as a module for $[Fe^{III}(L^2)Cu^{II}(Cl)_2(MeOH)]$. The redox responses in this bimetallic species are based on controlled oxidations and reductions of its fundamental components, i.e., the metal centers and the electroactive arms of the ligand.[10] Specific potentials trigger definite spin ground-state changes, as observed by EPR spectroscopy.

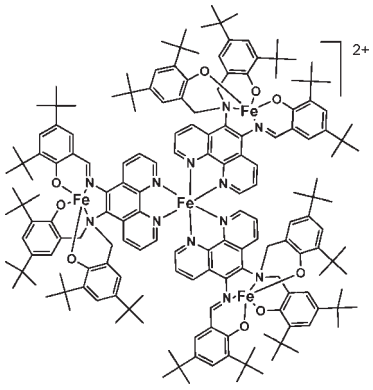

Figure 1. Modular discoid species $[Fe^{II}(Fe^{III}L^2)_3]^{2+}$.

In this account, we describe the synthesis and characterization of the tetrametallic $[Fe^{II}(Fe^{III}L^2)_3](PF_6)_2$ (Figure 1), along with studies on its electrochemical and surfactant properties.

This discoid molecule (oblate spheroid with $x = y > z$) is a first example that reconciles the use of *tert*-butyl groups to promote redox activity and surfactancy by enhancement of

*To whom correspondence should be addressed. E-mail: cnverani@chem.wayne.edu.

(1) (a) Bodenthin, Y.; Pietsch, U.; Moehwald, H.; Kurth, D. G. *J. Am. Chem. Soc.* **2005**, *127*, 3110. (b) Talham, D. R. *Chem. Rev.* **2004**, *104*, 5479.
(2) (a) Hoogenboom, R.; Fournier, D.; Schubert, U. S. *Chem. Commun.* **2008**, 155–62. (b) Verani, C. *McGraw-Hill Yearb. Sci. Technol* **2010**, 142.
(3) (a) Zhang, J.; Chu, B. W.-K.; Chu, Z. N.; Yam, V. W.-W. *Organometallics* **2007**, *26*, 5423.
(4) (a) Wassel, R. A.; Gorman, C. B. *Angew. Chem., Int. Ed.* **2004**, *43*, 5120. (b) Low, P. J. *Dalton Trans* **2005**, 2821.
(5) (a) Guerrero-Martinez, A.; Vida, Y.; Dominguez-Gutierrez, D.; Albuquerque, R. Q.; De Cola, L. *Inorg. Chem.* **2008**, *47*, 9131. (b) Wang, K.; Haga, M.-a.; Monjushiro, H.; Akiba, M.; Sasaki, Y. *Inorg. Chem.* **2000**, *39* (18), 4022.
(6) (a) Hindo, S. S.; Shakya, R.; Rannulu, N. S.; Allard, M. M.; Heeg, M. J.; Rodgers, M. T.; da Rocha, S. R. P.; Verani, C. N. *Inorg. Chem.* **2008**, *47*, 3119. (b) Shakya, R.; Imbert, C.; Hratchian, H. P.; Lanznaster, M.; Heeg, M. J.; McGarvey, B. R.; Allard, M.; Schlegel, H. B.; Verani, C. N. *Dalton Trans.* **2006**, 2517.
(7) Lanznaster, M.; Hratchian, H. P.; Heeg, M. J.; Hryhorczuk, L. M.; McGarvey, B. R.; Schlegel, H. B.; Verani, C. N. *Inorg. Chem.* **2006**, *45*, 955.
(8) Lanznaster, M.; Heeg, M. J.; Yee, G. T.; McGarvey, B. R.; Verani, C. N. *Inorg. Chem.* **2007**, *46*, 72.
(9) Elemental analyses gave lower than expected carbon contents for $[Fe^{II}(Fe^{III}L^2)_3](PF_6)_2$. Best results were obtained for $[Fe^{II}(Fe^{III}L^2)_3](ClO_4)_2$ ($C_{171}H_{213}Cl_2Fe_4N_{12}O_{17}$, MW = 3002.88) with C (calcd/exptl), 68.40/ 68.63; H, 7.15/7.27; N, 5.60/5.68.
(10) Davis, M. I.; Orville, A. M.; Neese, F.; Zaleski, J. M.; Lipscomb, J. D.; Solomon, E. I. *J. Am. Chem. Soc.* **2002**, *124*, 602.

Published on Web 07/21/2010

the species hydrophobic character. Thus, it supports the development of a modular approach to discoid multimetallic film precursors. Treatment of $[Fe^{III}L^2]$ with anhydrous $FeCl_2$ in a 3:1 ratio in methanol and under argon yielded the tetrametallic species $[Fe^{II}(Fe^{III}L^2)_3](PF_6)_2$ as a homogeneous microcrystalline solid. In spite of the apparent simplicity of the preparation, several attempts under aerobic conditions led to the formation of undesirable side products. This compound, as presently synthesized, was characterized by means of exact ESI mass spectrometry and elemental analysis.[9] Further characterization was obtained by comparative infrared, UV−visible, and XANES/EXAFS spectroscopies and electrochemical data between $[Fe^{II}(Fe^{III}L^2)_3](PF_6)_2$, the module $[Fe^{III}L^2]$, and the compound $[Fe^{II}(phen)_3](PF_6)_2$ (phen = 1,10-phenanthroline). The exact ESI-MS for the tetrametallic species (2802.3976 Da) in methanol exhibits peaks at m/z = 1401.69970 related to the bivalent cation $[Fe^{II}(Fe^{III}L^2)_3]^{+2}$ and 916.49504 associated with the module $[(Fe^{III}L^2)_3 + H^+]^+$. Comparison of the features present in the UV−visible spectra of $[Fe^{II}(Fe^{III}L^2)_3](PF_6)_2$, $[Fe^{III}L^2]$, and $[Fe^{II}(phen)_3](PF_6)_2$ in CH_2Cl_2 also permits one to ascertain the nature of the multimetallic species. The module $[Fe^{III}L^2]$ shows the expected intraligand $\pi\rightarrow\pi^*$ and N→Fe charge transfer bands at 281 and 333 nm (115 900 and 69 000 L $mol^{-1}cm^{-1}$), respectively. The phenolate-to-metal charge transfer bands[10] ($p\pi\rightarrow d\sigma^*$ and $p\pi\rightarrow d\pi^*$) appear at 411 and 463 nm (both at 27 500 L $mol^{-1}cm^{-1}$), thus unusually close to each other. This proximity is attributed to the five-coordination of the metal. The $[Fe^{II}(Fe^{III}L^2)_3](PF_6)_2$ species presents the analogous processes at 279 (249 700), 336 (96 000), and 486 nm (50 300 L $mol^{-1}cm^{-1}$), along with a new band at 525 nm (51 700 L $mol^{-1}cm^{-1}$). This new process is comparable to the metal-to-phenanthroline charge transfer present in $[Fe^{II}(phen)_3](PF_6)_2$ at 511 nm (9390 L $mol^{-1}cm^{-1}$), thus indicating the presence of all expected chromophores.[11] The IR spectrum of $[Fe^{II}(Fe^{III}L^2)_3](PF_6)_2$ presents peaks at 2870−2960 and 1605 cm^{-1} associated, respectively, with the *tert*-butyl and C=N groups in the module $[Fe^{III}L^2]$. Peaks associated with the counterion PF_6^- appear at 840 cm^{-1}. An equally prominent peak related to the out-of-plane deformation of the phenanthroline rings and enhanced through coordination is observed at 558 cm^{-1}. The XANES/EXAFS spectra of $[Fe^{II}(Fe^{III}L^2)_3](PF_6)_2$ and the module $[Fe^{III}L^2]$ are compared in Figure 2.

The edge position of $[Fe^{II}(Fe^{III}L^2)_3](PF_6)_2$ occurs at a slightly lower energy than that of $[Fe^{III}L^2]$ (7121.8(3) vs 7122.2(2) eV). A reduction from Fe(III) to Fe(II) should result in a lowering of the edge energy by ∼2−3 eV. This small shift in edge energy is, therefore, consistent with the presence of both trivalent and bivalent oxidation states, where the Fe(III) state is predominant. A pre-edge peak in the XANES of $[Fe^{II}(Fe^{III}L^2)_3](PF_6)_2$ occurs at 7113.0(1) eV, which corresponds to the parity-forbidden Fe(1s → 3d) transitions and has an area of 0.16(1) eV relative to the edge. These transitions gain intensity in noncentrosymmetric coordination environments through a dipole mechanism and are thus more intense in five- vs six-coordinate environments.[12] The Fe(1s → 3d) transition of $[Fe^{III}L^2]$ at 7113.2(1) eV has an area of 0.21(1) eV relative to the edge. Therefore, the average iron coordination environment is slightly more symmetric in $[Fe^{II}(Fe^{III}L^2)_3](PF_6)_2$ than in $[Fe^{III}L^2]$, suggesting that the multimetallic species contains both five- and six-coordinate iron centers. The EXAFS region of $[Fe^{II}(Fe^{III}L^2)_3](PF_6)_2$ was best modeled with iron surrounded by nitrogen and oxygen donors. Three shells are resolvable: one shell containing two short Fe−O scatterers at 1.84 Å, one shell containing three Fe−N or Fe−O scatterers at 1.96 Å, and one shell containing a single long Fe−N scatterer at 2.10 Å. This is consistent with the average iron environment predicted for $[Fe^{II}(Fe^{III}L^2)_3](PF_6)_2$.

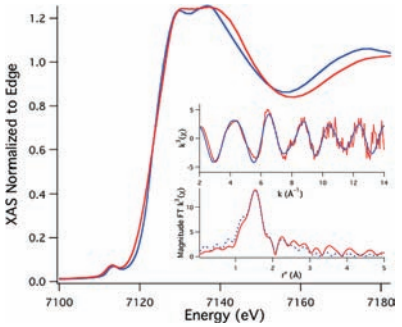

Figure 2. XANES region of the Fe K-edge XAS for $[Fe^{II}(Fe^{III}L^2)_3](PF_6)_2$ (red) and $[Fe^{III}L^2]$ (blue). Inset: EXAFS region for $[Fe^{II}(Fe^{III}L^2)_3](PF_6)_2$. Data (red) and simulation (blue). Shell 1 (Fe−O): n = 2, r = 1.839(6) Å, σ^2 = 0.0048(13) Å^2. Shell 2 (Fe−N): n = 3, r = 1.960(3) Å, σ^2 = 0.0010(5) Å^2. Shell 3 (Fe−N): n = 1, r = 2.104(13) Å, σ^2 = 0.0030(2) Å^2. Shell 4 (Fe−C): n = 4, r = 2.919(6) Å, σ^2 = 0.0053(8) Å^2. $E°$ = 7128.7 eV. ε^2 = 0.63.

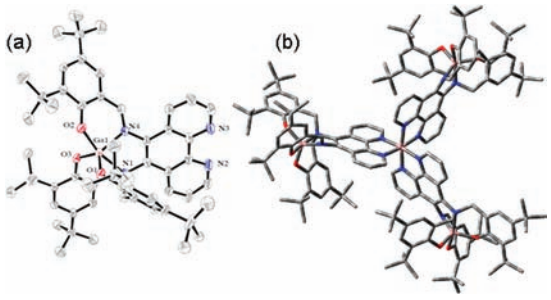

Figure 3. (a) ORTEP for $[GaL^2]$, Ga−O(3) = 1.828(3), Ga−O(1) = 828(3), Ga−O(2) = 1.899(3), Ga−N(4) = 1.975(4), Ga−N(1) = 2.266(4) Å. (b) MM-UFF model for $[Ga(GaL^2)_3]^{2+}$.

In spite of several attempts, the determination of the molecular structure for $[Fe^{II}(Fe^{III}L^2)_3](PF_6)_2$ via X-ray diffraction was not possible. The structure of the module $[Fe^{III}L^2]$ was published recently,[8] but attempts to use it as a starting point for calculations has proven to be nontrivial due to the large number of unpaired electrons at the iron centers.

Therefore, we obtained a crystal structure for the analogous compound $[Ga^{III}L^2]$.[13] The ORTEP representation is shown in Figure 3a with selected bond lengths. The similar nature of the gallium and iron structures is inferred by their neutral character, the identity of the ligand showing a monosubstituted amine N4 with a single phenolate appended,

(11) All expected chromophores: Braterman, P. S.; Song, J.-I.; Peacock, R. D. *Inorg. Chem.* **1992**, *31*, 555.

(12) (a) Roe, A. L.; Schneider, D. J.; Mayer, R. J.; Pyrz, J. W.; Widom, J. L.; Que, L., Jr. *J. Am. Chem. Soc.* **1984**, *106*, 1676. (b) Westre, T. E.; Kennepohl, P.; DeWitt, J. G.; Hedman, B.; Hodgson, K. O.; Solomon, E. I. *J. Am. Chem. Soc.* **1997**, *119*, 6297.

(13) $[Ga^{III}L^2]$: $C_{63}H_{80}GaN_7O_3$, M = 1053.06 Bruker P4/CCD (Mo/graphite), T = 208(2) K, triclinic, P(−1), a = 13.5969(18), b = 14.763(2), c = 15.893(2)Å, α = 113.395(4), β = 92.907(4), γ = 93.361(4)°, V = 2913.5(7) Å^3, Z = 2, D_{calc} = 1.200 Mg/m^3, abs. coeff = 0.522 mm^{-1}, 15 444 refls collected, 12 319 unique [R(int) = 0.042], θ = 2.04−28.31°, R1 = 0.0754, wR2 = 0.1707, GOF F^2 = 0.896 [$I > 2\sigma(I)$].

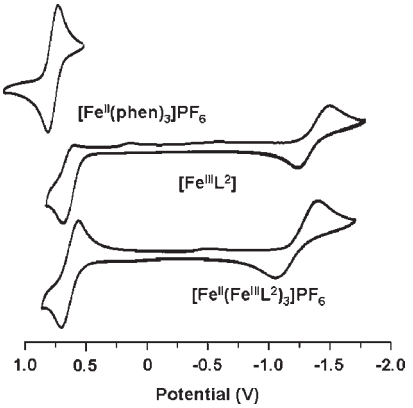

Figure 4. CVs of $[Fe^{II}(phen)_3](PF_6)_2$ (top), $[Fe^{III}L^2]$ (middle), and $[Fe^{II}(Fe^{III}L^2)_3](PF_6)_2$ (bottom) in dichloromethane, $TBAPF_6$ vs Fc^+/Fc.

whereas the vicinal amine N1 exhibits two of these groups. Furthermore, both species display a short bond length characteristic of a C=N imine group and a metal center that is five-coordinated in a N_2O_3 environment. On the basis of these similarities, a model $[Ga^{III}(Ga^{III}L^2)_3]^{3+}$ was built and its geometry minimized using the molecular mechanics UFF force field[14] available in the Gaussian 03 software package.[15] This model describes one possible isomer, shown in Figure 3b, in which one module displays the singly appended phenolate pointing upward while the two other modules point downward. Although several isomers are possible,[16] the one displayed is more stable by *ca.* 20 kcal/mol when compared to three other calculated geometries. In all cases, the models provide evidence for the discoid nature of the multimetallic species. On the basis of the similar ionic radii of gallium(III) (0.76 Å) and iron$_{ls}$(II) (0.75 Å), as well as in the already established similarities between the complexes of both metals coordinated to these pentadentate ligands, an estimated geometric radius from the central metal to the periphery is calculated to lie between 9.0 and 11.0 Å. Examination of the positions occupied by the *tert*-butyl groups attached to each phenolate reveals that the majority of these groups point outward conferring an enhanced hydrophobic cushioning which prevents the charged and hydrophilic discoid core from sinking into water and leads to a differentiated topology. The redox responsivity of $[Fe^{II}(Fe^{III}L^2)_3](PF_6)_2$ was assessed by cyclic voltammetry (CV, vs Fc^+/Fc). Comparison with the $[Fe^{III}L^2]$ module and with $[Fe^{II}(phen)_3](PF_6)_2$ allowed for attributions to the origin of the observed processes (Figure 4).

The CVs for the multimetallic species and the module display a cathodic wave for the process ascribed to the Fe^{III}/Fe^{II} couple. This process is anodically shifted in the tetrametallic species to $E_{1/2} = -1.24$ V and is less reversible (ΔE_p = 0.33 V; $|I_{pc}/I_{pa}| = 1.8$) than that of the module at $E_{1/2} = -1.37$ ($\Delta E_p = 0.25$ V; $|I_{pc}/I_{pa}| = 1.4$). The phenolate/phenoxyl oxidative process occurs for both $[Fe^{II}(Fe^{III}L^2)_3](PF_6)_2$ and $[Fe^{III}L^2]$ at *ca.* $E_{1/2} = 0.64$ V. Interestingly, an enhanced reversibility is observed in the multimetallic complex, as indicated by $|I_{pc}/I_{pa}| = 0.8$, compared to a value of 0.2 observed

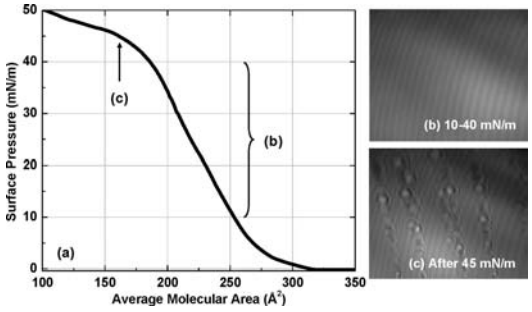

Figure 5. $[Fe^{II}(Fe^{III}L^2)_3](PF_6)_2$ at the air/water interface: (a) isothermal compression. Selected BAM images at (b) 10−40 mN/m and (c) collapse.

for the module. This profile might be associated with—or at least influenced by—the Fe(II)−phenanthroline core, because the metal-centered process for the unsubstituted $[Fe^{II}(phen)_3](PF_6)_2$ appears at $E_{1/2} = 0.77$ V ($\Delta E_p = 0.08$ V; $|I_{pc}/I_{pa}| = 1.1$). To evaluate the efficacy of the discoid design to act in hydrophobic precursors for film formation, compression isotherms plotted as surface pressure (mN/m) vs average molecular area (Å^2) were recorded at the air/water interface in a Langmuir−Blodgett trough at 23 °C, as shown in Figure 5a. The quality of the films was monitored during compression using Brewster angle microscopy (BAM), Figure 5b. The molecules of $[Fe^{II}(Fe^{III}L^2)_3](PF_6)_2$ start to interact with each other at the subphase at *ca.* 320 Å^2/molecule. The BAM images display a highly homogeneous film from 10 to *ca.* 40 mN/m, when a decrease in the slope of the isotherm coincides with the formation of linearly oriented Newton rings,[17] suggestive of a formal constant pressure collapse mechanism.[18] The average limiting area per molecule is 280 Å^2/molecule, thus with a radius of *ca.* 9.5 Å, in excellent agreement with the estimated radius of the $[Ga^{III}(Ga^{III}L^2)_3]^{3+}$ model.

In summary, we have reported on the tetrametallic complex $[Fe^{II}(Fe^{III}L^2)_3](PF_6)_2$ of discoid topology. The presence of metallic centers and ligand moieties such as phenolates and coordinated phenanthrolines extends the redox capabilities of this species. Along with its hydrophobic character, this species is a strong candidate for the formation of redox-responsive monolayer films. To the best of our knowledge, this is the first example of a discoid tetrametallic species in which the presence of *tert*-butyl groups concomitantly enforces redox activity *and* surfactancy. This result points to a general strategy in which a modular approach can be used to develop redox-active homo- and heterometallic film precursors of discoid topology. The synthetic approach and film transfer onto solid substrates are under investigation in our laboratories.

Acknowledgment. Support from the National Science Foundation (CHE-0718470, CHE-1012413), for C.N.V., and the WSU-IMR for F.D.L. is kindly acknowledged. We thank Dr. K. Kellersberger at Bruker Daltonics for the MS data.

Supporting Information Available: Synthesis details; X-ray structural determinations; molecular mechanics calculations; ESI-MS exact mass, infrared, XANES/EXAFS, and UV−visible spectra; electrochemistry; and isothermal compression and Brewster angle microscopy. This material is available free of charge via the Internet at http://pubs.acs.org.

(14) Rappé, A. K.; Casewit, C. J.; Colwell, K. S.; Goddard, W. A., III; Skiff, W. M. *J. Am. Chem. Soc.* **1992**, *114*, 10024.
(15) Frisch, M. J. *Gaussian 03*, revision D.01; Gaussian, Inc.: Wallingford, CT, 2004 (see Supporting Information for the full reference).
(16) Bergman, S. D.; Frantz, R.; Gut, D.; Kol, M.; Lacour, J. *Chem. Commun.* **2006**, 850.
(17) Galvan-Miyoshi, J.; Ramos, S.; Ruiz-Garcia, J.; Castillo, R. *J. Chem. Phys.* **2001**, *115*, 8178.
(18) (a) Kundu, S.; Datta, A.; Hazra, S. *Langmuir* **2005**, *21*, 5894. (b) Kundu, S.; Datta, A.; Hazra, S. *Phys. Rev. E* **2006**, *73*, 051608.